ALEX ZUNGER

Annales de la Société Scientifique de Bruxelles, T. 89, I, pp. 77-2212 (1975)

Super-Cell

SMALL PERIODIC CLUSTER CALCULATIONS ON PERFECT AND DEFECT SOLIDS

by

A. ZUNGER

Department of Theoretical Physics and Applied Mathematics
Soreq Nuclear Research Centre, Yavne, Israel
and Department of Chemistry, Tel Aviv University, Tel Aviv, Israel

ABSTRACT

We employ the small periodic cluster model for calculating electronic energy levels in both perfect solids and in point defect structures. The model is based on the representation of the one-electron energy spectrum of the crystal by the eigenvalues of a small periodic cluster of atoms arranged spatially according to the structure of the investigated system. To implement the calculations in practice semiempirical MO-LCAO approximations are used. The model is applied to study the properties of the perfect lattices of graphite and boron nitride, point defects in these structure and the band structure of solid HF and $(SN)_n$ metallic polymers. Good agreement with experiment is obtained.

I. INTRODUCTION

In view of the accumulation of rather extensive data on the electronic and dynamical properties of both perfect crystals and lattice imperfections, theoretical interest has been developed in calculational methods that treat both phenomena with similar methods [1]-[3]. While calculations that treat the perfect crystal yield theoretical values for crystal properties that are related to the *periodic* character (band structure, crystal conformation, etc.), point defect models tend to probe the properties that are related to the localized character of the defect (charge distribution around the defect site, local crystal deformation, etc.). The combination of both techniques enables the correlation between the defect levels and the perfect crystal band edges and also provides a good method for examining the quality of the potential used in the calculations.

II. THE SMALL PERIODIC CLUSTER (SPC) APPROACH

In the small-priodic cluster method one uses a real-space rather than a reciprocal-space approach to the determination of the one-electron eigenvalue-spectrum of periodic structures. Finite size periodic clusters of atoms are used to construct the electronic secular equations in the LCAO representation, yielding as a solution a subset of the infinite eigenvalue spectrum of the corresponding infinite solid. The method can be used to investigate both the band structure of a regular solid at discrete points in $\vec{k}$-space and the energy levels associated with point defects in the otherwise perfect solid.

Crystal orbitals $\psi_j(\vec{r})$ are constructed as linear superpositions of atomic orbitals $\chi_\mu(\vec{r} - \vec{R}_{n,\alpha})$ where μ denotes the atomic orbital quantum numbers ($\mu = 1s, 2s, 2p_x, 2p_y, 2p_z$, etc.) for the orbitals used :

$$\psi_j(\vec{r}) = N^{-1/2} \sum_{\mu=1}^{\sigma} \sum_{n=1}^{N} \sum_{\alpha=1}^{h} c_{\mu n\alpha}^{(j)} \chi_\mu(\vec{r} - \vec{R}_{n,\alpha}) \qquad (1)$$

N denotes the number of primitive unit cells and h indicates the number of inequivalent atoms in each primitive unit cell. The vectors $\{\vec{R}_{n,\alpha}\}$ indicate the position of the Nh atomic sites on a finite periodic array. The geometry of such an atomic cluster is conveniently described by an interatom distance matrix $D^{(Nh)}$ and three interatom direction-cosine matrices $E_x^{(Nh)}$, $E_y^{(Nh)}$ and $E_z^{(Nh)}$ where x, y and z indicate some arbitrary directions. These are constructed in the following way : A central Born-von Karman (BVK) cell is built. This cell is then extended in space by translating it in the x, y and z directions. Each atom in the central cell is allowed to interact with its neighbors, either inside the cell or outside it, up to a maximal range $R_c(N, h)$. The range $R_c(N, h)$ is chosen so that each atomic species on a given sublattice in the central BVK cell, experiences an identical crystalline coordination. The elements of the distance and direction cosine matrices, indicate the intra-cell and inter-cell distances and orientations used to established the periodicity. The Brillouin zone (BZ) constructed from these small periodic clusters, contain N discrete points in $\vec{k}$-space. The energies of the various $h\sigma$ crystals bands at these N points can be calculated by solving the eigenvalue problem associated with an Nh-atom pseudomolecule

with geometry defined by $D^{(N\lambda)}$, $E_x^{(N\lambda)}$, $E_y^{(N\lambda)}$ and $E_z^{(N\lambda)}$ and with the representation given in Eq. (1) for the trial vectors. This amounts to the calculation of the electronic eigenvalue problem of

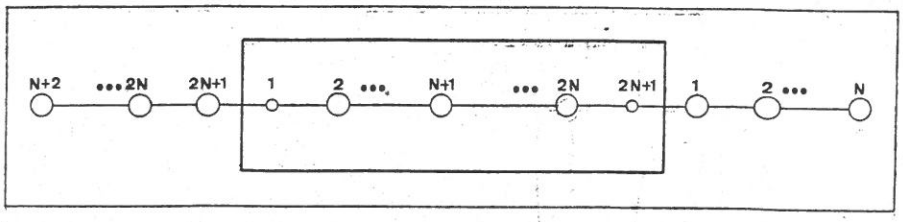

Fig. 1.
Construction of the small periodic cluster,
a) Linear chain of $2p + 1$ atoms,

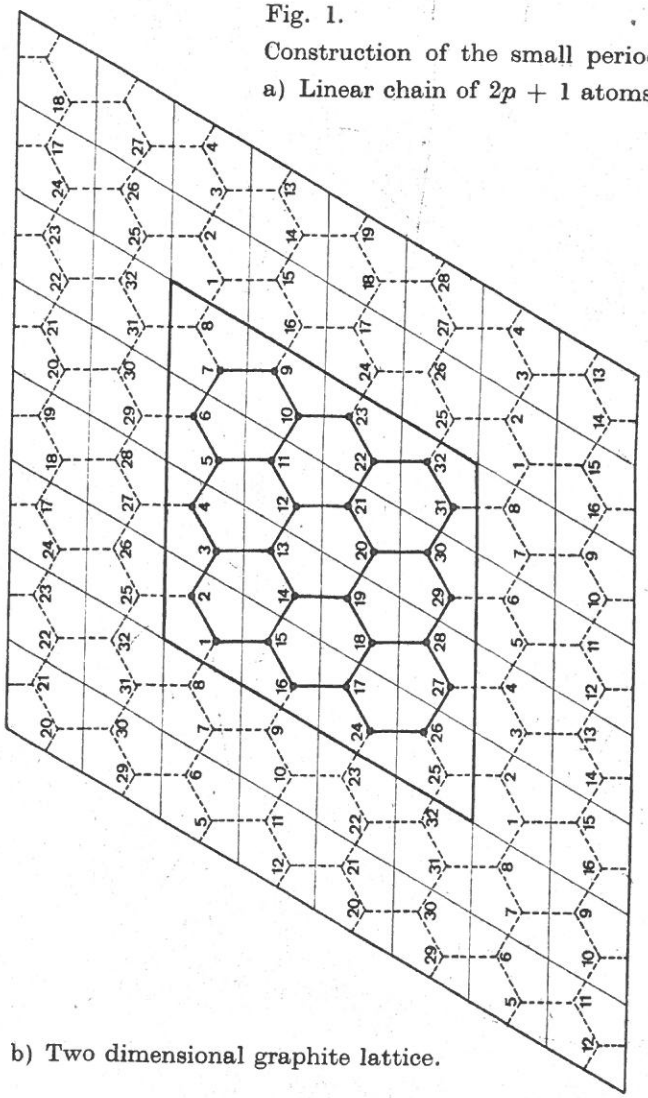

b) Two dimensional graphite lattice.

the central BVK cell that is embedded in the field of all other cells produced by translating it through space.

Fig. 1 demonstrates two simple cases where the interaction geometry is constructed to yield periodic clusters. In the first example, the central BVK cell consists of a linear one-dimensional chain of $N = 2p + 1$ atoms ($h = 1$). This is extended by the atoms labelled 1 to p on one side and by the atoms labelled $2p + 1$ to $p + 1$ on the other side. When the maximal interaction range is taken to be $R_c(N, 1) = pa$, where a is the nearest neighbor distance, each atom in the central cell experiences an identical coordination. In the second example, the hexagonal two-dimensional graphite structure is considered. The central BVK cell now consists of a $p \times p$ array of primitive unit cells each with $h = 2$ atoms ($N = p^2$, a total number of $2p^2$ atoms). The central cell is extended by $p/2$ (for even p) or by $p1/2$ (for odd p) primitive cells in the plane directions. The eigenvalue problem associated with the central BVK cell is now defined as the solution of the LCAO secular equations related to the $2p^2$ atoms with interaction range $p.a$.

The variational equations are :

$$\sum_{\mu=1}^{\sigma} \sum_{n=1}^{N} \sum_{\alpha=1}^{h} [F^{\alpha,\beta}_{\mu n,\lambda m} - S^{\alpha,\beta}_{\mu n,\lambda m} E_j] C^{(j)}_{\mu n \alpha} = 0 \qquad (2)$$

where the matrix elements are given by :

$$F^{\alpha,\beta}_{\mu n,m\lambda} = \langle \chi_\mu(\vec{r} - \vec{R}_{n,\alpha}) \mid \hat{F} \mid \chi_\lambda(\vec{r} - \vec{R}_{m,\beta}) \rangle \qquad (3)$$

$$S^{\alpha,\beta}_{\mu n,\lambda m} = \langle \chi_\mu(\vec{r} - \vec{R}_{n,\alpha}) \mid \chi_\lambda(\vec{r} - \vec{R}_{m,\beta}) \rangle$$

and $\hat{F}$ is the Hartree-Fock operator. When an explicit form is used for $\hat{F}$, the $F^{\alpha,\beta}_{\mu n,\lambda m}$ elements are given by :

$$F^{\alpha,\beta}_{\mu n,\lambda m} = H^{\alpha,\beta}_{\mu n,\lambda m} + \sum_{\mu' s,\lambda' t} \sum_{\alpha'\beta'} P^{\alpha'\beta'}_{\mu' s,\lambda' t} [(\mu n_\alpha \lambda m_\beta \mid \mu' s_{\alpha'} \lambda' t_{\beta'}) - \frac{1}{2} (\mu n_\alpha \lambda' t_\beta \mid \lambda m_\beta \mu' s_{\alpha'})] \qquad (4)$$

where the core-Hamiltonian matrix element is given by :

$$H^{\alpha,\beta}_{\mu n,\lambda m} = \langle \chi_\mu(\vec{r}_1 - \vec{R}_{n,\alpha}) \mid -\frac{1}{2} \nabla_1^2 - \sum_{S,A} \frac{Z_A}{\vec{r}_{s,1} - R_A} \chi_\lambda(\vec{r}_1 - \vec{R}_{m,p}) \rangle \qquad (5)$$

and the two-electron matrix elements are :

$$(\mu n_\alpha, \lambda m_\beta \mid \mu' s_{\alpha'}, \lambda' t_{\beta'}) =$$

$$= \langle \chi_\mu(\vec{r}_1 - \vec{R}_{n,\alpha}) \chi_\lambda(\vec{r}_1 - \vec{R}_{m,\beta}) \left| \frac{1}{\vec{r}_{12}} \right| \chi_{\mu'}(\vec{r}_2 - \vec{R}_{s\alpha'}) \chi_{\lambda'}(\vec{r}_2 - \vec{R}_{t\beta'}) \rangle \quad (6)$$

where Z_A is the nuclear charge. The elements $P^{\alpha'\beta'}_{\mu' s \lambda' t}$ of the charge matrix are defined by the expansion coefficients of Eq. (1) by :

$$P^{\alpha',\beta'}_{\mu' s \lambda' t} = \sum_j^{\sigma_\alpha} n_j \, C^{(j)*}_{\mu' s \alpha'} \, C^{(j)}_{\lambda' t \beta'} \quad (7)$$

where σ_α denotes the highest occupied level in the ground state and n_j is the occupancy number.

When $\hat{F}$ is replaced by some effective one-electron Hamiltonian, as is done in the extended Huckel [4] (EXH) theory, the $F^{\alpha,\beta}_{\mu n,\lambda m}$ elements are given by :

$$F^{\alpha,\beta}_{\mu n,\lambda m} = S^{\alpha,\beta}_{\mu n,\lambda m} [I^\alpha_\mu + I^\beta_\lambda] \frac{G}{2} \quad (8)$$

where $S^{\alpha,\beta}_{\mu n,\lambda m}$ denotes the overlap integral, I^α_μ and I^β_λ denote the orbital energy for orbitals μ, λ situated at sites α and β respectively, and G is the empirical Wolfgang-Helmholtz parameter. Equation (2) is solved with the elements given in Eq. (3) by either using the self-consistent form of Eqs. (4)-(7) or the form given in Ed. (8) for the matrix elements. To facilitate computations, the INDO approximations [5] to equations (4)-(6) are adopted in the former case. The empirical constants appearing in this approximation are the core energies I^α_μ and the bonding parameter $\tilde{\beta}$.

In the case of a perfect periodic structure, the eigenvectors and eigenvalues obteained, could be analyzed in terms of the wave vector $\vec{k}_n$, by recognizing that :

$$C^{(j)}_{\mu n\alpha} \equiv C^{\bar{\mu}\bar{n}\bar{\alpha}}_{\mu n\alpha} = C^{\bar{\mu}\bar{\alpha}}_{\mu\alpha}(\vec{k}_{\bar{n}}) \, e^{i\vec{K}\bar{n}\cdot\vec{R}\bar{n}} \equiv C^{\gamma}_{\mu\alpha}(\vec{k}_{\bar{n}}) \, e^{i\vec{K}\bar{n}\cdot\vec{R}_n} \quad (9)$$

$$E_j \equiv E_{\bar{\mu}\bar{n}\alpha} = E_\gamma(\vec{k}_{\bar{n}}) \quad (10)$$

where the band index γ ranges from 1 to σh and $\vec{k}_{\bar{n}} = \frac{2\pi}{N\vec{a}} \bar{n}$ for $\bar{n} = 0, 1, N - 1$. Thus, the band structure $E_\gamma(\vec{k}_{\bar{n}})$ is obtained for N $\vec{k}_{\bar{n}}$ points in the BZ. The charge matrix (Eq. 7) is expressed in this representation by :

$$P_{\mu\alpha\lambda\beta} = \sum_{\vec{K}_s} P_{\mu\alpha\lambda\beta}(\vec{k}_s) \quad (11)$$

where

$$P_{\mu\alpha\lambda\beta}(\vec{k}_s) = \sum_{\gamma}^{occ} n_\gamma \, C^{\gamma *}_{\mu\alpha}(\vec{k}_s) \, C^{\gamma}_{\lambda\beta}(\vec{k}_s) \qquad (12)$$

The diagonal element of (11) is the μ orbital charge on atom α due to all $\tilde{\sigma}_n$ occupied bands.

The total energy of the $\tilde{\sigma}_{0c}$ bands is obtained in the Hartree-Fock representation by :

$$E_{tot} = \frac{1}{2} \sum_{\mu n, \lambda m, \alpha\beta} P^{\alpha,\beta}_{\mu n,\lambda m} \left[H^{\alpha,\beta}_{\mu n,\lambda m} + F^{\alpha,\beta}_{\mu n,\lambda m} \right] + \sum_{A<B} \frac{| \, Z_A Z_B \, |}{R_A - R_B} \qquad (13)$$

and in the effective-one-electron Hamiltonian picture, by

$$E_{tot} = \sum_{j}^{occ} n_j E_j = \sum_{\gamma}^{occ} \sum_{\vec{k}_s} n_j E_\gamma(\vec{k}_s) \qquad (14)$$

where n_j is the occupation number of level j.

In the defect problem, we either change the chemical identity of a specific atom in the central BVK cell (substitutional impurity) or reject this atom (point vacancy) and repeat the solution of Eq. (2). The spectrum obtained corresponds to a superlattice of defects with a defect-defect distance greater than $R_c(N, h)$.

The convergence problems associated with the energy solution in the SPC approach involving the self-consistent scheme (Eq. 4-7) are :

(a) Convergence of the lattice sums i.e. the magnitude of $R_c(N, h)$ used to calculate the elements in Eq. (3).

(b) Convergence of reciprocal space sums i.e. the number of $\vec{k}_n$ values entering in the calculation of the charge matrix in Eq. (11)

(c) Convergence of the results as a function of the size σ of the basis set employed. In most computations a minimal valence basis set will be used neglecting the contribution of the higher orbitals.

Convergence problems (a) and (b) could be reduced to one if one uses the *maximal* range $R_{max}(N, h)$ permitted for an Nh-atom cluster. In this case, for a given h, both $R_c(N, h)$ and the number of $\vec{k}_n$-

points yielded in the SPC representation, are uniquely determined by N. In the non-self consistant approach (using Eq. 8), the matrix element $F^{\alpha,\beta}_{\mu n,\lambda m}$ depends only on the orbital pair $(\mu n\alpha)$ and $(\lambda m\beta)$, consequently the convergence problem (b) does not occur in evaluating these elements. The total energy (Ed. 14) depends however on the number of $\vec{k}$-points included in a particular cluster representation.

After one establishes a reasonable convergence in the sums $a - b$ for a particular choice of the porbital energies I^{α}_{μ} (in EXH and INDO schemes) and a bonding parameter $\tilde{\beta}$ (INDO cheme), the resulting wave functions are subjected to a Mulliken population-analysis to yield atomic charges. Similarly, the wave functions are used to compute the total electronic charge density $\rho(\vec{r})$ that is used in turn to compute the electrostatic Poisson potential $V(\vec{r}, \vec{R})$ by solving :

$$\nabla^2 V_{elec}(\vec{r}) = -4\pi\rho(\vec{r}) \qquad (15)$$

$$V_{tot}(\vec{r}, R) = -V_{elec}(\vec{r}_i) + \sum_a \frac{Z_A}{|R - \vec{r}|}$$

When the basis functions used can be expanded in gaussians, eq. (15) can be analytically solved [3]. The potential $V_{tot}(\vec{r}, R)$ is used to characterize the potential rearrangements introduced by a defect in the crystal. It can also be used in other problems where a crystalline potential is required.

The crystal conformation under static equilibrium is studied minimizing $E_{tot}(\vec{d})$ with respect to the unit cell parameters denoted by the components of $\vec{d}$. This is done by solving iteratively the equation :

$$\delta\vec{d} = -A\Delta_{\vec{d}} E_{tot}(\vec{d}) \qquad (16)$$

Near the minimum, the first derivative method (eq. 16) is non convergent and a simple mapping procedure is used. This results in the equilibrium unit all parameters $\vec{d}_{eq}$ and the lattice cohesion $E_{tot}(\vec{d}_{eq}) - E_{tot}((\infty)$ relative to its isolated ocnstituents. At the vicinity of equilibrium, the second derivative of $E_{tot}(\vec{d})$ with respect to symmetrical crystal coordinates is numerically evaluated, to yield force constants.

The calculation procedure used with the SPC method consists of the following steps :

Perfect lattice :

a) One chooses a cluster size that is sufficient to establish the convergence criterion previously discussed to within a prescribed tolerances.

b) For each set of the empirical parameters $\{I_\mu^\alpha, G\}$ in the EXH method and $\{I_\mu^\alpha, \tilde{\beta}\}$ in the INDO method, one obtains in a single solution, a subset of energy eigenvalues at some high symmetry points in the BZ. When sufficient experimental data concerning band-to-band transition energies, band widths, work function and atomic charges exists, a least-square procedure is used to obtain the ebst agreement with the experimental band structure and charges by adjusting these parameters. These have been previously parameterized to yield various molecular properties [5]. The values of these parameters arrived at in such procedures [5] are used as an initial guess for the refinement process.

c) The crystal equilibrium unit cell parameters and cohesive energy are calculated by the minimization procedure indicated in Eq. (16). The results are compared with crystallographic and thermochemical data. Similarly, force constants (and possibly elastic constants) are evaluated from second derivatives and compared with values deduced from phenomenological lattice dynamical treatments.

Since the SPC method yields only a discrete energy subsets the density of states and photoelectron emission energy profile, can be calculated only via a low-resolution histogram. However, if the results of step b) and c) are satisfactory, one can use either a conventional tight-binding calculation with the parameters arrived at in those steps or a perturbative $\vec{k} \cdot \vec{p}$ expansion to obtain quasicontinuous results. This is unnecessary if only discrete optical data are considered.

When satisfactory results are obtained for the perfect lattice, one proceeds with the examination of the properties of imperfections in these solids. The procedure used is :

a) The cluster size is gradually increased to obtain stability of the defect levels with respect to the interaction radius. At this limit, defect-defect interactions in this defect superlattice representation are suppressed and the isolated defect limit is approached.

b) The features introduced by the defect on the crystal orbitals are examined. These include the charge distribution in the defect orbitals (if this orbital is singly occupied, the wave functions obtained can be used to calculate EPR hyperfine splitting constants), the energy separation between the defect oribtals and the band edges (to be compared with thermoluminescence and photoconductivity data) and the defect formation energy. Similarly, lattice relaxation around the defect site could be examined.

The main disadvantages of the SPC method are :

1) Since translational symmetry is not used to reduce the size of the secular equations, one has to treat relatively large matrices. On the other hand, problems in which this symmetry is lost (point defects, calculation of vibrational force constants, etc.), are conveniently treated.

2) The defect one-electron energies obtained correspond to a defect-superlattice rather than to an isolated defect.

3) Due to computational difficulties involved with big clusters, semi-empirical rather than *ab-initio* LCAO methods, are used.

- The main advantages of the method are :

1) Relations between perfect and defect crystal energy spectrum, can be conveniently examined.

2) A single calculation for the perfect crystal yields several evenly spread $\vec{k}$-points in the BZ. These are usually high symmetry points whose energy is related to many optical data. Parametrization of the semi-empirical scheme can thus be conveniently performed.

3) Since translational symmetry (Bloch conditions) is not imposed explicitely on the wave function one can easily examine problems where this symmetry is lacking, such as the stability of a given crystal structure against atom displacements, point defect problems, etc.

In what follows, we will briefly describe the results obtained by applying the SPC method to some simple solids. These include the band structure and vacancy formation in graphite and hexagonal boron nitride and determination of some electronic and

dynamical properties of the protons in the hydrogen-bonded HF crystal. and Peierls instability in the metallic $(SN)_n$ polymer.

III. RESULTS

A. *Boron nitride*

The band structure of the perfect lattice of hexagonal boron nitride (point group D_{3h}) was previously [6] calculated using the SPC approach with the self-consistent iterative extended Huckel [7] scheme. The results obtained by using the EXH method are shown in Table I and compared with the available experimental data and with the scaled tight binding calculation of Doni et al. [8] and the OPW calculation of Nakmanson [9]. The band structure along the

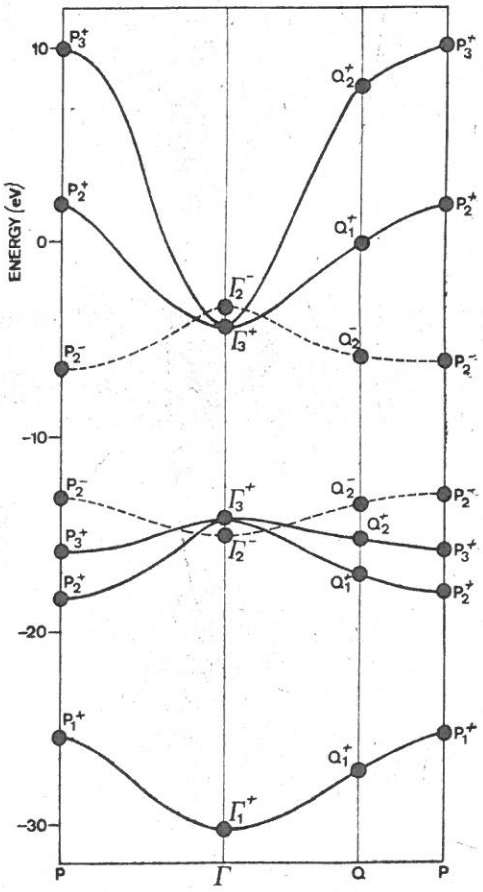

Fig. 2. — Band structure of hexagonal boron nitride, calculated by the SPC method, using the EXH approximation.

P — l — Q — P line is shown in Fig. 2. The agreement with experimental data is seen to be quite good.

The nitrogen vacancy problem has been investigated [19] using both EXH and IEXH methods. The results compared favorably with thermoluminiscence and EPR data previously published [20]. Recently, it was demonstrated that carbon atoms have a significant role in determining the nitrogen vacancy EPR and optical properties [21]. We have calculated the electronic spectrum of an SPC of boron nitride replacing a nitrogen atom by a carbon. The results are schematically shown on Fig. 3. It is seen that the carbon atom introduces 3 additional levels in the energy gap : a doubly degenerate c_α state an a singly degenerate a_α stte. These are strongly localized around the carbon site. The separation form of the c_α state from the edge of the conduction band (4.87 ev) and from the

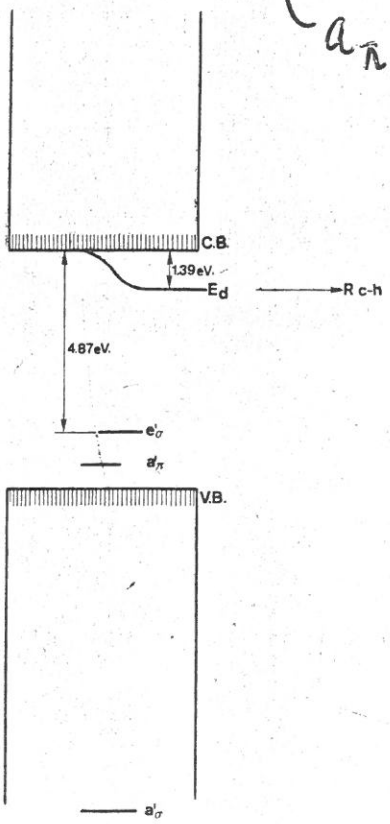

Fig. 3. — Defect levels in boron nitride.

valence band (1.4 ev) is consistent with the experimental determination [21], [22]. When the carbon atom is vertically displaced from its substitutional site (increasing R_{c-h} in Fig. 3), an additional π level splits from the conduction band. This level is characterized by a symmetrical charge distribution on the three boron atoms surrounding the defect. The calculated square of the LCAO coefficient on these boron atoms is 0.020. This compares favorably with the value of 0.0187 determined from the experimental hyperfine splitting constant [21] using the Hartree-Fock value of $\langle r^{-3} \rangle$ [23]. The separation of the defect level from the edge of the conduction band is calculated to be 1.1 ev .Lattice relaxations around this site stabilize the system and lower the defect level to within 1.38 ev. from the conduction edge. This compares reasonably well with the experimental value [20], [21] of 1 ± 0.1 ev determined from the temperature variation of the EPR signal and from thermoluminescence.

B. *Graphite*

Results for the band tructure of perfect graphite solid using standard parameters in the EXH method have been published [19], [6]. Since considerable experimental data exists on band-to-band transitions in graphite, it is possible to improve the agreement between the SPC results and experiment by varying the parameters I^{α}_{μ} of the EXH expression (Eq. 8). The results of such a procedure are shown in Table II. The band structure along the P — Γ — Q — P line is shown in Fig. 4. The results were obtained using the parameters $I^{c}_{2s} = 21{,}4^{(4)}_{ev}$, $I^{c}_{2P_\lambda} = I^{c}_{2P_\lambda} = 0.8\, I^{c}_{2P_s}$ with $I^{c}_{2P_\lambda} = -11.4^{(4)}_{ev}$ and G = 1.85. Good agreement is obtained with most of the experimental data.

Next, the problem of carbon vacancy in graphite is studied by the SPC method. It is observed that upon rejecting a carbon atom from the hexagonal skeleton, some new one-electron energy levels appear. In particular, the point Γ_{α}^{1+} in the perfect lattice band structure is transformed into a a' type state (D_{3h} point symmetry) and the doubly degenerate $\Gamma_{\varepsilon}^{(+)}{}_{h}$ state is transforme to a e' orbital. These are the levels predicted to appear in a graphite vacancy structure by the « defect molecule » model of Coulson et al. [34]. It is shown here that if one uses the SPC representation to describe the perfect lattice states (rather than just four atoms as is done

TABLE I

Calculated and experimental properties of two-dimensional Boron-nitride using the EXH approximation

Property	Experimental	Experimental Method	EXH	Empirical (8) T — B	OPW (9)
Valence band width (ev)	18.6 [11]	X-ray emission	18.1	13.6	27.8
Eg (ev)	5.4 [11]-5.8 [12]	Absorption	5.49	5.4	3.6
$Q_2^- \rightarrow Q_3^-$ (ev)	6.2 [11]	Electron energy loss	6.3	6.6	3.1
$E^{++} - E_2$ (ev)	19.4	ESCA	19.0	16.2	34.
$Q^+ \rightarrow Q^+$ (ev)	14.1 [11]	Electron energy loss	15.1	16.8	
$Q^+ \rightarrow Q^+$ (ev)	9.4 [11]		9.4	9.7	
Binding energy (ev)	6.6 [11]	Thermochemistry	—	—	
R_{BN} (Å)	1.446 [11]	Crystallography	1.443	—	—
Qne (e)	0.45 [11]	NQR	0.35	—	—
*k*stret dyn/cm	8.3×10^5 [11]	Band spectra	13.1×10^5		

TABLE II

Calculated and experimental properties of two-dimensional graphite

Property	Experimental	Experimeâtal method	EXH	Empirical T — B [24]	Ab-Initio T — B [25]	OPW [26]	Pseudo potential [27]
Ionization Potential (ev)	4.8 [28]	Thermoionic Emission	8.3	8.95	8.84		
π-band-width (ev)	~ 5.5 [29]	Soft X-rays	5.6	4.0	7.35	7.05	7.0
Total-Valence width (ev)	15±3 [29], 31±2 [30]	Soft X-rays [29], ESCA [30]	22.4	14.0	19.3		10.
Binding energy (ev)	7.4 [31]	Thermochemistry	6.8				
$\Gamma^+_{3g} \rightarrow \Gamma^+_{3u}$ (ev)	5.95 [32], 6.2 [33]	Reflectivity	6.0	6.0	12.2	18.7	9.
$Q^-_{2g} \rightarrow Q^-_{2u}$ (ev)	4.6 [34], 5.11 [33]	Reflectivity	4.8	4.5	4.6	5.2	3.9
$Q^+_{1g} \rightarrow Q^-_{2u}$ (ev)	∿ 16 [34]	SEE	15.2	13.3	16.5		
$Q^+_{2u} \rightarrow Q^+_{2g}$ (ev)	∿ 15 [34]	SEE	14.8	15.8	16.3		
Req. (Å)	1.42 [35]	Crystallography	1.41				
k dyn/cm	1.80×10^6 [36]	Compressibility	2.9×10^6				
— « γ_0 » integral (ev)	2.7 [37] — 3.2 [38]	Magnetic [37] Susceptibility [22] dH — VA [38]	2.42	0.74		2.58	

we obtain $E_v = 12.84$ ev. Optimizing now the total energy with respect to relaxation of the bond lengths around the vacant site, we obtain $E_v^{rel} = 12.25$ ev for a contraction of 4.2 % of the R_{cc} bond length. Using the experimental value of E_s [31] we obtain $E_{vf} = 4.81$ ev. This compares favorably with the experimental values 3.3 ± 0.9 ev [40] and 5.5 ± 1 cv [42] and with the observe d average basal plane contraction of $\frac{\Delta a}{a} > 2$ % [43]. The details of the vacancy levels and other defects in graphite are being further studied using the SPC model.

C. *Hydrogen fluoride*

The band structure of solid HF calculated by the INDO method in the one dimensional chain approximation (point group c_{2v}) is shown in Fig. 5. No optical data is yet available to compare the calculated band structure.

The crystal conformation of the zigzag HF chains has been a controversial subject for long time [44]-[48]. Crystallographic maesurements [44], Raman frequency assignment [45] and residual entropy measurements [46] have been used to investigate the proton positions. We utilize here the SPC model for a HF chain having an intramolecular distance $R_{HF} \equiv d$, an intermolecular distance a and a chain angle α. 11 orders of neighbors were found to be sufficient to assure the convergence of the lattice sums and the $\vec{k}$-sums. We use the optimization method denoted in Eq. (16) to minimize the total crystal energy. Using a fixed R_{FF} distance (experimental value 2,49 Å [44]) we find $d_{eq} = 1{,}015$ Å and $\alpha = 122^{o}$ and a cohesive energy of 17.9 kcal/mole. The experimental α value is 120 ° [44]. This results suggests that the protons assume asymmetric positions ($d_{\alpha\alpha} \neq R_{FF}/2$) as suggested by residual entropy

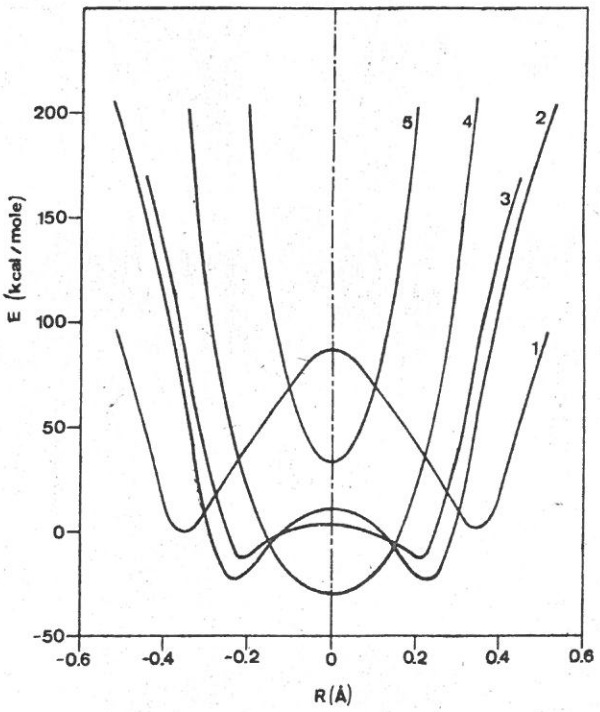

Fig. 6. — Potential for proton displacement in solid HF.

measurements [46]. The intramolecular bond length d is increased by $\sim$ 0,01 Å relative to the isolated molecule value. The crystal potential energy as a function of proton positions is shown in Fig. 6 where the characteristic double-well is obtained. The energy required to form an ionic Bjerrum defect (by translating a specific proton to the opposite part of the potential well) is calculated to be 83.9 kcal/mole.

The vibrational force constants for solid HF are computed from the total Hartree-Fock energy by computing numerically the second derivatives. This results in 7.2×10^5 dyn/cm and 6.1×10^5 dyn/cm ofr the asymmetric and symmetric stretching force constants, respectively. The experimental values deduced from IR and Raman spectre [45] are 6.5×10^5 and 5.3×10^5 dyn/cm respectively.

D. *Polysulfur nitride* $(SN)_n$

Polysulfur nitride $(SN)_n$ has been shown to be a one dimensional metallic conductor even at Helium temperatures and to exhibit a negative Seebeck coefficient [47]. The origin of this metallic behavior has been previously assigned to ~~a small extent of bond alternation~~ [48]. Recent crystallographic studies [49] have shown that $(SN)_n$ is characterized by an alternating structure with $R_{SN}^{(1)} = 1{,}54$ Å and $R_{SN}^{(2)} = 1{,}74$ Å alternatively and chain angles around 120°. We have applied the SPC method to study the band structure of $(SN)_n$ chains. We use $2s$, $2p$ orbitals for nitrogen and $3s$, $3p$ and $3d$ orbitals for sulfur and employ the CNDO/2 SCF-LCAO scheme to calculate the eigenvalue spectrum. The band structure for the lowest valence bands, is shown in Fig. 7. Experimental $R_{SN}^{(1)(2)}$ values are employed and $\alpha = 180°$ is used for simplicity. It is evident that the highest populated band is only half occupied in the ground state resulting thereby in metallic behavior. The Fermi energy is calculated to be 7.5 ev. The corresponding value for the chain having the experimental chain angles is 7.45 ebv.

The problem of bond alternacy in the $(SN)_n$ structure, is investigated in the SPC method by calculating the first derivative of the total Hartree-Fock energy with respect to Δ (defined as $R_{SN}^{(2)} = R_{SN}^{(1)} - \Delta$) for several $R_{SN}^{(2)}$ values. It is observed that for $1.7 \leqslant 106$ Å a negative value is obtained, indicating that the structure with $\Delta \neq 0$ is more stable than the $\Delta = 0$ structure.

.5097a
24.4.75

over this RSN range. This agrees with recent experimental data [49] and not with the earlier determination [50].

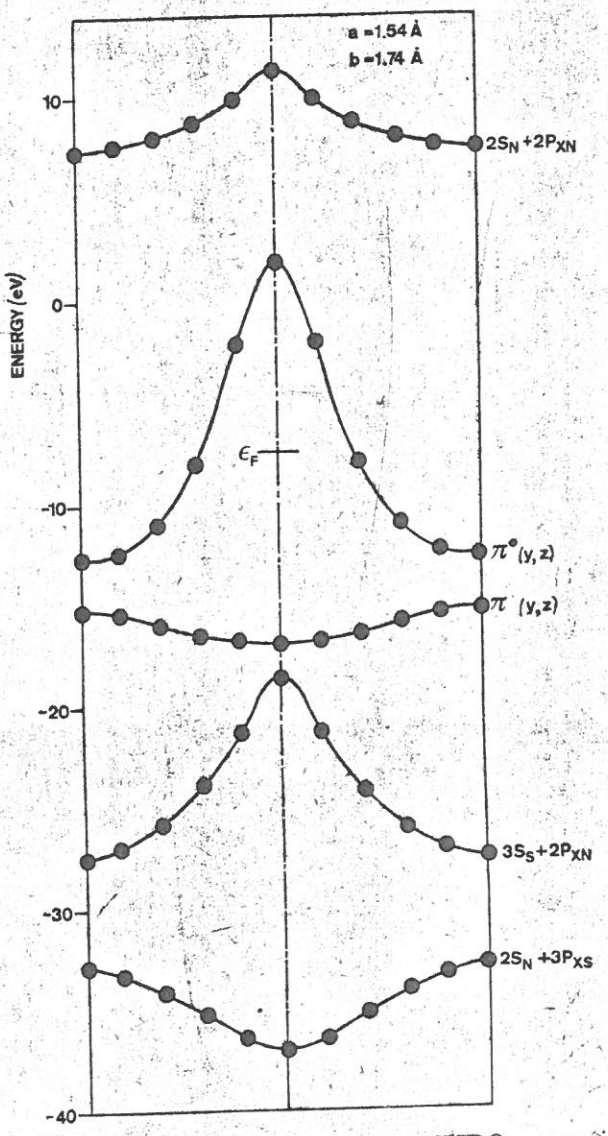

Fig. 7. — Band structure of the $(SN)_n$ chain (CNDO approximation).

The problem of non-occourence of a Peierles instability in the one-dimensional $(SN)_n$ chain was investigated by searching a superlattice 95 of conformational changes that will both create a gap in the half-occupied band and lower the total Hartree-Fock energy. No such instability could be

REFERENCES

[1] R. P. Messmer and G. D. Watkins, *Phys. Rev. B.*, **7**, 2568 (1973),

[2] F. P. Larkins, *J. Phys. C.*, **4**, 3065 (1971),

[3] A. Zunger, *J. Phys. C.*, **7**, 76 (1974).

[4] R. Hoffman, *J. Chem. Phys.*, **39**, 1397 (1963).

[5] J. A. Pople and D. L. Beveridge, Approximate M. O. Theory (McGraw Hill, N.Y.) 1970.

[6] A. Zunger, *J. Phys. C.*, **7**, 96 (1974) & A. Zunger and A. Katzir, *Phys. Rev. B.* (in press) (1974).

[7] R. Rein, H. Fukuder, H. Win, G. A. Clark and F. E. Harris in Quantum Aspects of Heterocyalic Compounds in Chemistry and Biochemistry, Proc. Jerusalem Symp. (Israel Academy of Science and Humanities), p. 86 (1969).

[8] E. Doni and G. P. Paravicini, *Nuovo Cim.*, **63** A, 117 (1969).

[9] M. S. Nakhmanson and V. P. Smirnov, *Sov. Phys. Solid. St.*, **13**, 2673 (1972).

[10] V. A. Formichev, *Sov. Phys. Solid St.*, **13**, 754 (1971).

[11] S. Larach and R. E. Shrader, *Phys. Rev.*, **107**, 68 (1956).

[12] W. Baronian, *Mater. Res. Bull.*, **7**, 119 (1971).

[13] R. Vilanov, *C. R. Acad. Sci. Paris*, B **272**, 1066 (1971).

[14] K. Hamrin, G. Johansson, V. Gelins, C. Nordling and K. Siegbahan, *Phys. Soc.*, **1**, 277 (1970).

[15] Janaf International Thermochemical Tables, LA-2368 (1965).

[16] R. S. Pease, *Acta Crystallogr.*, **5**, 356 (1952).

[17] A. H, Silver and P. J. Bray, *J. Chem. Phys.*, **32**, 788 (1960).

[18] J. Goubean, Boron-Nitrogen-Chemistry Advances in chemical series No. 42, *American Chemical Society*, p. 87 (1964).

[19] A. Zunger, *J. Chem. Phys.*, in press (1974).

[20] A. Katzir, J. T. Süss and A. Halperin, *Phys. Lett..*, A **41**, 117 (1971).

[21] A. W. Moore and L. S. Singer, *J. Phys. Chem. Solids*, **33**, 343 (1972).

[22] A. Katzir, J. T. Suss, A. Zunger and A. Halperin, *Phys. Rev. B.* (in press) 1974.

[23] C. M. Hurd and P. Coodin, *J. Phys. Chem. Solids*, **18**, 573 (1967).

[24] F. Bassani and G. P. Parravicini, *Nuovo Cim.*, **50**, 95 (1967).

[25] G. S. Painter and D. E. Ellis, *Phys. Rev. B.*, **1**, 4747 (1970).

[26] M. Tsukada, K. Nakao, Y. Uemura and S. Nagai, *Phys. Soc.-Japan*, **37**, 54 (1972).

[27] W. V. Haeringen and H. G. Junginer, *Solid St. Comm.*, **7**, 1723 (1969).

[28] V. S. Fomenko, Handbook of Thermionic Properties Plenum, N. Y. (1966).

[29] F. C. Chalkin, *Proc. Roy. Soc. Lon.*, A **194**, 47 (1948).

[30] J. M. Tomas, E. L. Evans, M. Barber and P. Swift, *Trans. Faraday Soc.*, **67**, 1875 (1971).

[31] G. Glockler, *J. Chem. Phys.*, **22**, 159 (1954).

[32] A. Balzarotti and M. Grandolfo, *Phys. Rev. Lett.*, **20**, 9 (1968).

[33] D. L. Greenaway, G. Harbeke, F. Bassani and E. Tossatti, *Phys. Rev.*, **178**, 1340 (1969).

[34] R. F. Willis and B. Fitton, *Surface Sci.*, **9**, 651 (1971).

[35] W. N. Reynolds in Physical Properties of Graphite, Elsevier (1968).

[36] L. Pauling, *Proc. Nat. Acad. Sci. U.S.A.*, **56**, 1646 (1966).

[37] J. W. McClure, *Phys. Rev.*, **104**, 666 (1956).

[38] J. W. McClure, *Phys. Rev.*, **108**, 612 (1957).

[39] C. A. Coulson, M. A. Herrnaes, M. Leal, E. Santos and S. Senet, *Proc. Roy. Soc. Lond.*, A **274**, 461 (1963).

[40] J. H. W. Simmons, Radiation Damage in Graphite, Pergamon, p. 43 (1965).

[41] C. Baker and A. Kelly, *Nature* (Lond.), **193**, 735 (1962).

[42] W. N. Reynolds and P. A. Thrower, *Phil. Mag.*, **12**, 573 (1965). Later the procedure used by these authors for computing the experimental E_{vf} value was criticized (ref. 43) since no allowance was made for the C-axis spacing. Since we are employing a two dimensional model, we refer to values of Reynolds and Thrower, for consistency.

[43] R. W. Hanson and W. N. Reynolds, *Carbon*, **3**, 177 (1965).

[44] M. Atoji and W. N. Lipscomb, *Acta Cryst.*, **7**, 173 (1954).

[45] J. S. Kittelberger and D. F. Hornig, *J. Chem. Phys.*, **46**, 3099 (1967).

[46] J. H. Hu, D. White and H. L. Johanston, *J. Amer. Chem. Soc.*, **75**, 1232 (1953).

[47] V. V. Walatka, M. M. Labes and J. H. Perlstein, *Phys. Rev. Lett.*, **31**, 1139 (1973).

[48] D. Chapman, R. J. Warn, A. G. Fitzgerald and A. D. Joffe, *Trans. Faraday Soc.*, **60**, 294 (1964).

[49] M. Boudeulle and P. Michel, *Acta Crystallogr. Sect.*, A **78**, S 199 (1972).

[50] M. Goehring, *Quart. Rev. Chem. Soc.*, **10**, 437 (1950).

[51] A. Zunger, J. chem. phys. (In Press).